INVESTIGATION BY SIMULATION AND EXPERIMENTAL VERIFICATION OF MPPT ALGORITHMS FOR PARTIALLY SHADED STAND ALONE PHOTOVOLTAIC SYSTEMS

D.V.Ravikumar[1] Dr.V.Rajasekaran[2]

[1]Department of Electrical and Electronics Engineering, Adithya Institute of Technology, Coimbatore, Tamilnadu, India.
E-mail: dvravikumareee@gmail.com

[2]Department of Electrical and Electronics Engineering, PSNA College of Engineering and Technology, Dindigul, Tamilnadu India. E-mail:rajsekaranvm@gmail.com

Abstract: *The availability of solar energy varies widely with ambient temperature, different atmospheric and partially shaded conditions. The generated photovoltaic (PV) voltage of each module becomes unequal. Under partially shaded conditions, when the PV module characteristics get more complex with multiple peaks of output power, in such systems, analyzing the performance of maximum power points tracking (MPPT) schemes for independent control of each of the PV modules becomes essential. In this system, the experimental implementation and the MATLAB / SIMULINK based simulations are compared with fuzzy logic control (FLC) and adaptive neuro-fuzzy inference system (ANFIS) MPPT algorithms in terms of parameters like global peak, tracking speed, power extraction, and harmonic analysis under various partial shading conditions. In this topology, each cascaded H-bridge inverter (CHBMLI) unit is connected to an individual PV module through an interleaved soft switching boost inverter (ISSBC). This topology permits independent control of each PV module to operate at the maximum power point. It also offers another advantage such as lower ripple current and switching loss compared to the conventional boost inverter. The performance of the selective harmonic elimination (SHE) PWM, with a trained ANN sub system for a single phase CHBMLI to generate balanced output voltage even under partially shadowed condition of PV modules is analyzed. The results are evaluated by simulation and experimental implemented on a 300W PV panel prototype with the microcontroller platform. The simulation and hardware results show that ANFIS algorithm is more efficient than the FLC algorithm.*

Key words: Photovoltaic (PV) system, Maximum power point tracking (MPPT), Microcontroller, Interleaved softswitching boost inverter (ISSBC), cascade H-bridge inverter (CHBMLI).

1. Introduction

Photovoltaic (PV) systems are used for power generation since many decades. Today, with the focus on greener sources of power a PV system has become an important source of power for a wide range of applications. Improvements in converting light energy into electrical energy as well as the cost reductions have helped create this growth. Even with higher efficiency and lower cost, the goal remains to maximize the power from the PV system under various lighting conditions. The main applications of PV systems are either stand-alone (water pumping, domestic applications, street lighting, electric vehicles, military and space applications) [1] or grid-connected configurations. The efficiency of a PV plant depends on three factors like the translation efficiency (very low 9-15%), especially under low irradiation conditions, temperature and shaded condition. Improving the efficiency of the PV panel depends on the technology available; it may require better components that can increase radically the cost of the installation. Moreover, The P-V and I-V characteristic curves of a solar cell are highly dependent on the solar radiation and temperature values [2]. In general, there is a unique point on the P-V or I-V curve, called the maximum power point (MPP), at which the entire PV system operates with maximum efficiency and produces its maximum output power.

The performance of a photovoltaic module is highly affected by the partial shaded condition. This results in the shaded cell to dissipate power as heat and causing hot spots that can harm the PV module by degrading the cell and in cases the whole system by affecting its performance [3]. Therefore, in order to minimize the effect of partial shading, a diode is connected in parallel to the cell to allow the current to bypass the shaded cell. However, it will also result in a decrease in power extraction efficiency of the PV module [4]. Many MPPT techniques have been reported in the literature such as perturb and observation, incremental conductance, fuzzy logic based controller etc. [5] - [8].

In this paper FLC and ANFIS [9] MPPT algorithm being used to extract the maximum DC power from PV module by ISSBC. The generated DC power is converted into AC, in order to be used in a standalone system. In recent times, multilevel inverter topologies have received more attention to the use in PV applications [10]. The output waveforms are much improved over conventional inverter. However, there is always a chance of unbalanced input DC-link voltages in CHBMLI when fed from PV module [11]. However, if the voltage balance is not perfectly accomplished, the modulation methods may create an error in the output voltage. This leads to harmonics in the output voltage and current of the multilevel inverter. To overcome the difficulties, in this paper, single phase selective harmonic elimination ANN integrated modulation technique is proposed and verified.

2. Stand alone PV system

The block diagram of the proposed topology for ISSBC and CHBMLI based stand-alone PV system is shown in Fig.1.Each H-bridge inverter is fed from an individual photovoltaic module through a DC-DC inverter integrated with FLC and ANFIS MPPT algorithm. The output of the single phase SHE trained ANN unit has been applied to the CHBMLI to achieve a balanced output with improved power quality even under non-ideal condition of PV module.

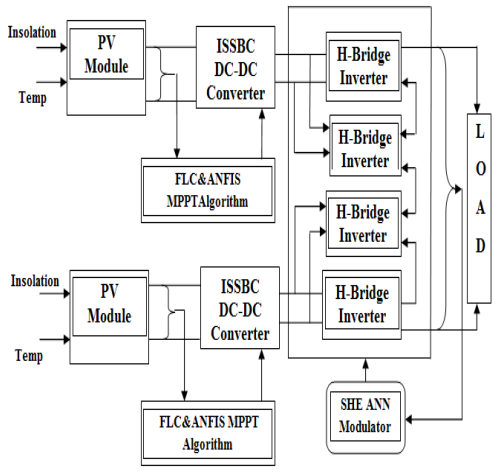

Fig.1. General Diagram of load connected photovoltaic system

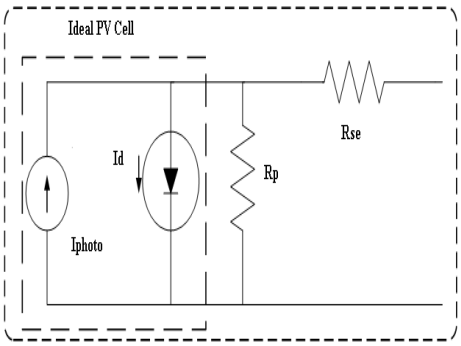

Fig.2. Equivalent model of the PV panel

Table 1. PV module parameters

Parameter	
Maximum Power (P_{max})	150W
Voltage at Pmax (V_{mp})	34.5V
Current at Pmax (I_{mp})	4.35A
Open-circuit voltage (V_{oc})	43.5V
Short-circuit current (I_{sc})	4.75A

3. PV array modeling and simulation

The PV array used in the proposed system is 72 multi-crystalline silicon solar cells in series and able to provide 150W of maximum power [12]. In this model, a PV cell is represented by a current source in parallel with a diode and a series resistance as shown in Fig. 2. The basic current equation is given in Eq. (1).

$$\mathbf{I = Ipv,cell - I0,cell}\left[\mathbf{exp}\frac{qv}{akT}\mathbf{- 1}\right] \quad (1)$$

Where I_PCell = current generated by the incident light (directly proportional to sun irradiation), I_0Cell = leakage current of the diode, q = electron charge 1.6021×10-19 C, k = Boltzmann constant (1.38×10-23 J/K), T = Temperature of the PN junction, a = Diode ideality constant. Practically the PV array comprised with many PV cells connected in series and parallel. This makes some additional parameters to be added with the basic Eq. (1). The modified equation is shown in the Eq. (2) and Eq. (3).

$$\mathbf{I = Ipv - I0}\left[\mathbf{exp}\left[\frac{V+\mathbf{R}sI}{V_a}\right]\mathbf{- 1}\right]\mathbf{-}\frac{V+RsI}{Rp} \quad (2)$$

$$I\mathbf{pv}=\left(I\mathbf{pv,n}+\mathbf{K}1\Delta T\right)\frac{G}{Gn} \quad (3)$$

The parameters of the solar array at nominal operating conditions are shown in Table 1.

4. MPPT control algorithms

The MPPT algorithm is used for extracting the maximum power from the PV module and passes it on to the load. A DC-DC inverter serves the purpose of transferring maximum power from the solar PV module to the load. By changing the duty cycle the load impedance, as seen by the source, is varied and matched at the point of the peak power with the source so as to transfer the maximum power.

4.1 FLC MPPT algorithm

The FLC MPPT algorithm is used to ISSBC to compensate the output voltage of PV system to keep the voltage at the value which maximizes the output power. The fuzzy logic controller consists of three basic elements, namely fuzzification, rule base inference engine and defuzzification (Chokri Ben Salah et al., 2011).

Fuzzification comprises the process of transforming numerical crisp inputs into linguistic variables based on the degree of membership to certain sets. The fuzzification variables are logical decision framed in inference engine block and delivers linguistic output. Defuzzifier is used to convert linguistic fuzzy sets to actual value. In this system assigned in terms of several linguistic variables by using seven fuzzy subsets, which are denoted by NB (negative big), NM (negative medium), NS (negative small), Z (zero), PS (positive small), PM (positive medium) and PB (positive big). In this paper the fuzzy inference rule is carried out by using Mamdani's method and the defuzzification use the centre of gravity to compute the output of this FLC which is the duty cycle. The two FLC input variables are the error *E(k)* and change of error *CE (k)* at sampled times *k* defined in Eq. (4).

$$E(k)=\frac{P\mathbf{pv}(k)\ -\mathbf{Ppv}(\mathbf{k}-\mathbf{1})}{V\mathbf{pv}(k)\ -\mathbf{Vpv}(\mathbf{k}-\mathbf{1})} \quad (4)$$

$$\mathbf{CE}(k)=\mathbf{E}(k)\ -\mathbf{E}(\mathbf{k}-\mathbf{1}) \quad (5)$$

where *P(k)* and *V(k)* are the instant power and voltage of the photovoltaic system respectively *E* (*k*) is zero at the maximum power point of PV array. The input *E(k)* shows if the operation point at the instant k is located on the left or on the right of the MPPT on the PV Characteristic while the input *CE (k)* expresses the moving direction of this point(Mohamed Salhi et al.,2011).

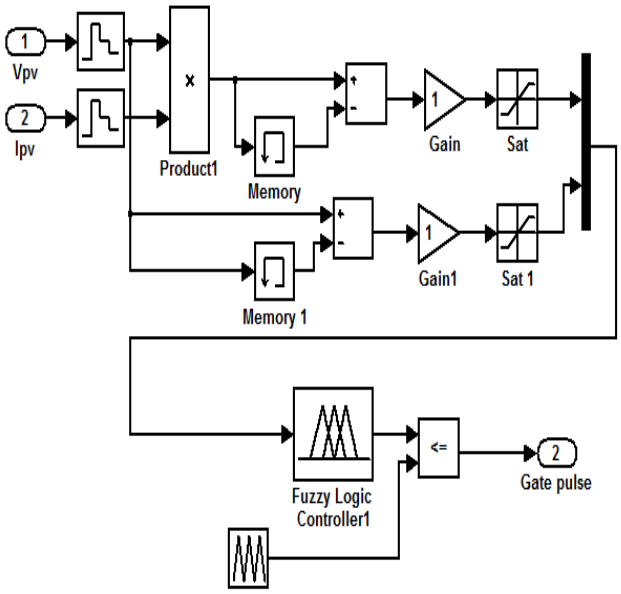

(a)

4.2 ANFIS MPPT algorithm

The ANFIS system is used to formulate the neural network architecture in the inference engine of a Fuzzy controller. The functional block diagram and structure of ANFIS is shown in Fig.4 (a-b). The structure comprises of three distinct layers namely input layer, hidden layer and output layer.

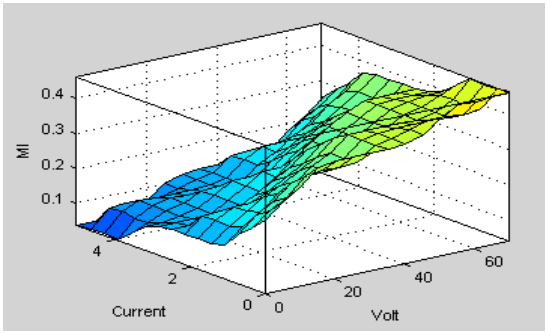

(b)

Fig.3. (a) FLC MPPT control system (b) FLC surface output

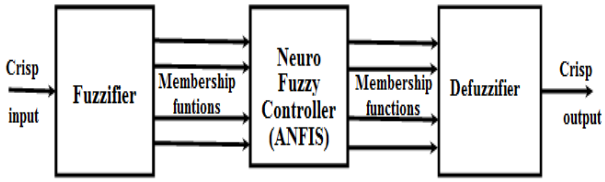

(a)

The ANFIS controller implemented in this article is of the model described as above whose fuzzifier section comprises of the input signals error *(e)* and change in error signal *(ce)* whose membership functions are selected as Gaussian membership function and are classified into seven functions namely Negative Big (NB); Negative Medium (NM); Negative Small (NS); Zero (ZE); Positive Small (PS); Positive Medium (PM) and Positive Big (PB).

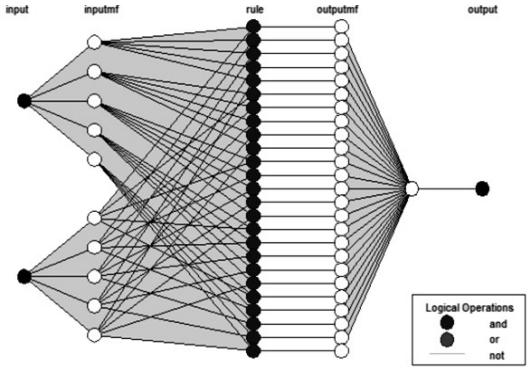

(b)

Fig.4. (a) Adaptive neuro fuzzy control system (b) ANFIS rule base model structure

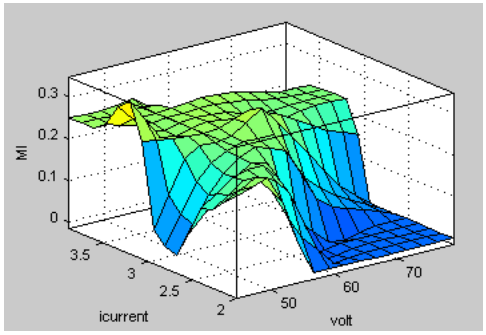

Fig.5. ANFIS Surface view

The defuzzifier of the ANFIS is the output function that is the modulation index *(d)*. The input membership functions are mapped to the output membership function by 49 rules through grid partitioning method using the FIS generator in MATLAB Simulink. The *250* data sets to train ANFIS is obtained from workspace from the previous FLC MPPT algorithm model in which data's namely PV voltage and current and the corresponding modulation index *(MI)*. The learning data trained through back propagation technique for 50 epochs for minimum error tolerance. The network training is performed repeatedly until the performance indexes $E_p = \left(V_{\mathbf{ref}} - \mathbf{V_{pv}}\right)^2$ $Ep = (Vref - Vpv)2$ $E_p = (V_{ref} - V_{pv})^2$ reduce below a specified value ideally to zero. In other words when $E_p \to 0$ $Ep \to 0$ leads to $(V_{ref} - V_{pv})^2 \to 0$ $\left(V_{\mathbf{ref}} - \mathbf{V_{pv}}\right)^2 \to 0$, then the trained

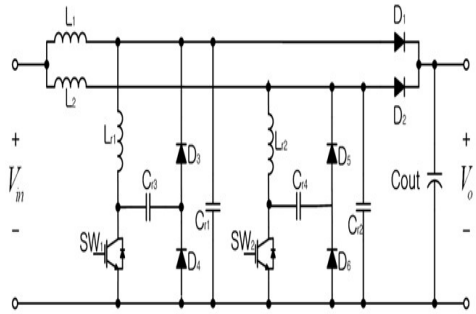

Fig.6. Interleaved Soft-Switching Boost Inverter (ISSBC)

ANFIS connecting weights are adjusted in such a way that the estimated array voltage is identically equal to the MPP voltage [16]. The trained surface rule phase

view shown in Fig.5, the trained data set exports the simulation and observes the performance different partial shading condition.

5. Soft switching boost inverter

It serves as a suitable interface for PV cells to convert low voltage, high current input into a high voltage low current output. In this study based on MPPT algorithm the micro controller generates a gate signal to control the interleaved boost inverter and compare the energy output two MPPT algorithms. Fig. 6 shows the functional diagram of an ISSBC, the interleaved boost inverter consists of two single phase boost inverters that are connected in parallel and inverters operating 180 degrees out of phase with 30 kHz switching frequency. It is pointed out that in interleaved inverter mode 60 kHz effect is achieved by phase shifting of the two 30 kHz switching signals. The input current is the sum of the two-inductor currents, I_{L_1} **and** $\mathbf{I}_{L_2}$ $I_{l1} \wedge I_{l2}$ shown in Fig.7. Because the inductor ripple currents are out of phase, they cancel each other and the input-ripple current reduce to 12% of that of a conventional boost inverter. The best input-inductor-ripple-current cancellation occurs at 50% duty cycle. Hence, the design value of the duty ratio is 0 to 0.5 in this system. Therefore, the interleaved inverters have the wider continuous current mode, the reduced input current ripple and output voltage ripple, and lower switching losses, therefore the output voltage of the solar cell can be boosted with high efficiency [18].

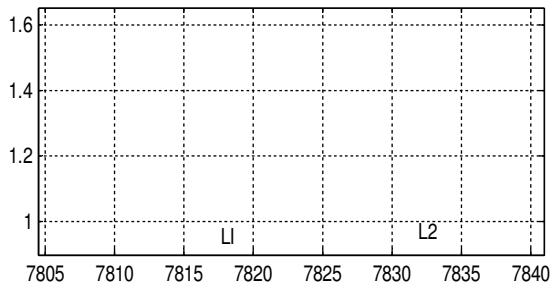

Fig.7. ISSBC Main inductor L1 and L2 current simulation waveform

6. Single phase CHBML inverter

The cascaded multilevel inverter is composed of a number of H-bridge inverter units with separate DC source for each unit and can be connected in cascade to produce a near sinusoidal output voltage waveform using the proper modulation scheme shown in Fig.8. There are different switching strategies implemented for minimization and elimination of harmonics [19] - [21].

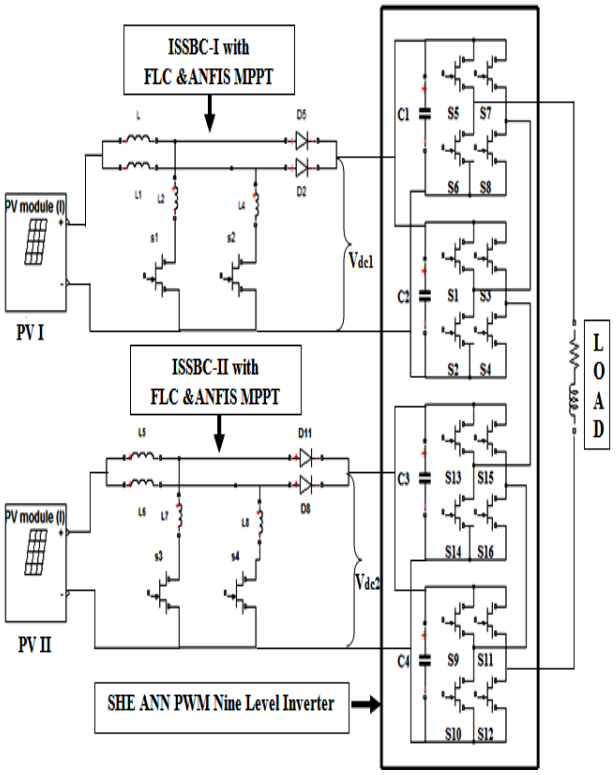

Fig.8. Schematic diagram of cascaded multilevel inverter based stand alone PV system

The control of the multilevel inverter with both the SPWM and SVPWM methods, the unbalance of the DC voltages is the most important areas of concern. If this voltage balance is not perfectly achieved, the modulation method creates errors in the modulated output voltage. This fact leads to distortion in the output voltage waveform of the multilevel power inverter. As in the proposed topology of CHBMLI, each H-bride cell is fed from an individual PV module. There is always a chance of voltage unbalance because of the partial shadow effect on any of the PV modules.

$$V_{ab}(wt) = \sum_{n=1,5,7,11\ldots}^{\infty} \left[\frac{4}{\pi.n} \left(V_{pv1} \cos(n.\alpha_1 \right) + V_{pv2} \cos(n.\alpha_2 \right. \quad (6)$$

In this paper selective harmonic elimination pulse with modulation technique is implemented to generate the switching duty cycle for CHB inverter. The equation (6) shows the contents of the output voltage at infinite frequencies, the module voltage V_{pv1}-V_{pv2} are associated to their respective switching angle α_1- α_2. These trigonometric transcendental equations can be solved by GA and implemented to find the switching angle (offline) for a set of predetermined modulation indices to get the required fundamental output voltage in a nine level cascaded multi level inverter. The switching angles (α_1, α_2) lie in between 0 and $\pi/2$. As explained in section 4, collected the set of data trained in ANN Simulink tool and exported to the system. A sample data set is presented in Table 2. The ANN is trained to output the set of angles for each input voltage situation.

Table 2. ANN training data for CHBMLI

Input voltage	Switching angle(°)
[25 25 25 25]	[0.4 9.8 19.4 0.41]
[25 29 35 39]	[5.0 16.5 19.8 35.7]
[35 37 39 40]	[7.2 28.9 41.4 52.1]
….	…..
[35 36 38 39]	[21.5 37.5 51.7 58.3]
[40 42 42 42]	[37.5 70.8 58.3 39.0]

7. Simulation Results

The simulink software validates the performance of the MPPT techniques under different operating conditions. The PV module parameters are obtained from the 150-Watts multicrystalline PV Module technical data sheet. All algorithm tests are performed considering the same temperature and irradiation steps. Such parameters are considered in the Standard Test Condition (STC): 1000W/m^2 and cell temperature of 25°C.

The simulation block diagram is shown in Fig.9. First, the characteristics of the PV module are validated and connected with stand-alone system then the performance of the MPPT techniques under various conditions is evaluated to investigate the output power efficiency.

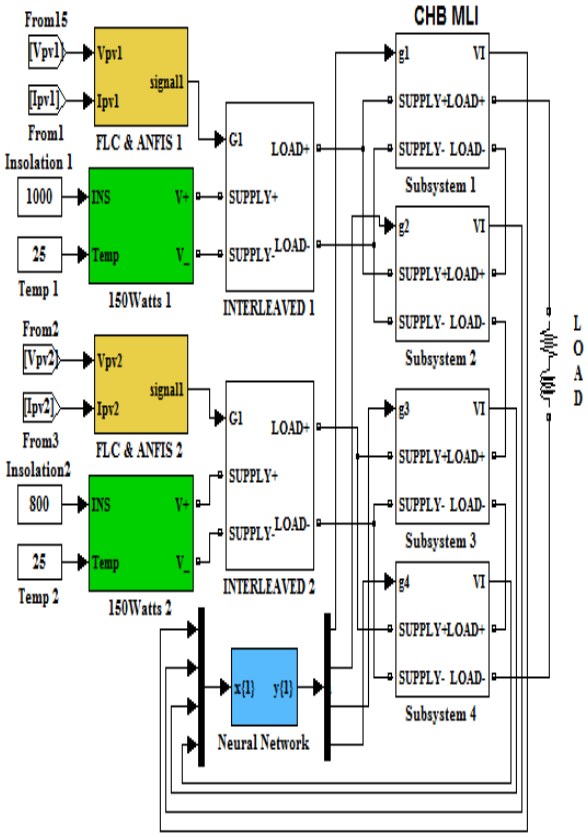

Fig.9. Simulation block diagram of the system

The simulation validation of PV module and inverter results of the I-V and P-V characteristics of PV module as a function of irradiation and temperature shown in Fig. 10-11.

It can be observed quite similar to the PV module as per data sheet. In order to achieve the maximum power point of PV modules, FLC and ANFIS MPPT controller has been developed using Matlab Simulink model. The simulation result is presented for the following different configurations.

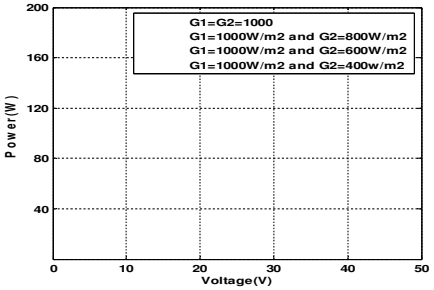

Fig. 10. P-V Curve at 25°C

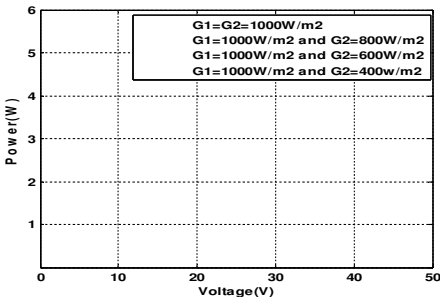

Fig. 11. I-V Curve at 25°C

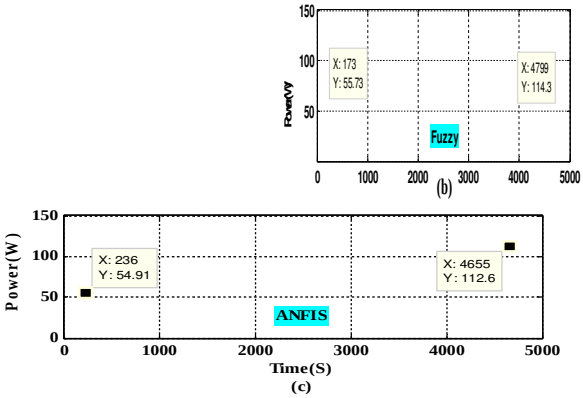

Fig.12. Power outputs of the MPPTs by dynamic behavior at 25°C (a) Radiation step (600-10000 W/m^2, (b) FLC and (c) ANFIS.

7.1. Effect of Changing the Solar Radiation

Simulations are carried out for the two techniques under dynamically changing solar irradiations at temperature of 25°C. Fig. 12 (a-c) shows output power of sudden changes in solar irradiation from 600-to1000 W/m^2. In this analysis, the two techniques are able to extract the MPP.

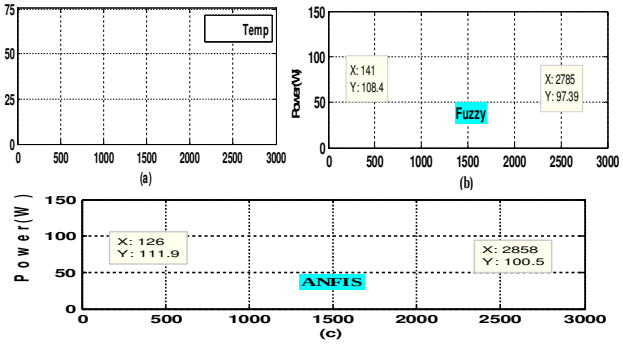

Fig.13. Power outputs of the MPPTs by dynamic behavior constant Radiation 900W/m^2 (a) Temperature step (25-50°C), (b) FLC and (c) ANFIS.

FLC power equal to 54.91 watts at 600W/m^2, algorithms respond lesser to reach new MPP sudden change in irradiation. The ANFIS power extracted 59.2 watts at 600W/m^2 fast response to reach the new MPP after solar irradiation changes. Higher power extracted from ANFIS algorithm compared to FLC also gives a fast steady state response with less oscillation.

7.2. Effect of Change in Temperature

This simulation is carried out to illustrate the performance of the MPPT methods under constant solar irradiation of 900W/m^2 and changes in temperature from 25°C to 50°C. The temperature has a slight effect on the cutoff circuit current. However, the open circuit voltage decays quickly as the temperature increases. Fig. 13 (a-c) shows the corresponding PV output power, during slowly occurring as well as sudden changes in temperature respectively, With the FLC the maximum power extracted is 110 Watts; when compared to ANFIS the FLC does not converges to the globally maximum power point. The ANFIS exhibits fast response and also converges to the globally maximum power point with slight fluctuations and highest PV output power in the face of the dynamics of temperature.

Corresponding output voltage change is also small but biggest voltage and current ripple error, its value is about 0.59% of nominal voltage. Fig. 14 (a-b) shows steady state performances of two MPPT control algorithms. With solar irradiation of 600W/m2, the overshoot voltage and current settling time is 0.0028s for FLC algorithms. ANFIS gives faster response of 0.0013s compared FLC algorithm.

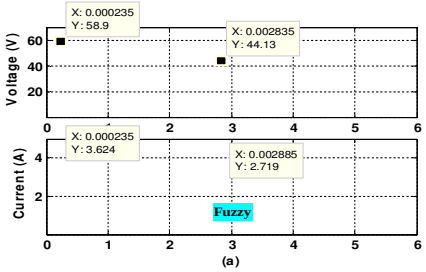

7.3. Transient response of PV output voltage and current

In this analysis, steady state performance parameters are ripple amplitudes of array load current

and voltage, overshoot and settling time at the disturbance of insulation and temperature. The PV systems operating in MPPT conditions by a change in duty cycle based on control algorithm, a value of the increment or decrement of 0.001 each step is followed.

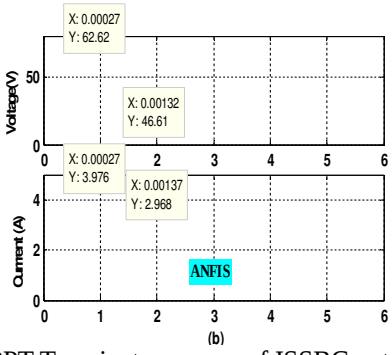

Fig.14. MPPT Transient response of ISSBC output voltage and current Irradiation 600 W/m^2 and temperature 25°C (a) FLC (b) ANFIS

7.4. Tracking factor evaluation of MPPT algorithms

The transmitted energy is essential for the evaluation of the PV cell as an energy source; a very important measure is the tracking factor, which is the percentage of available energy that is converted. The ripple voltage in steady state is also very important, as there is a limit of ripple so that the panel will remain effective at the MPP.

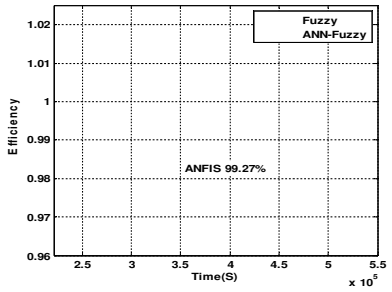

Fig.15. TF curves of MPPTs

In this system ISSBC reduces the ripple content both on the source and load side, reduce current stresses in the switches and improving the tracking factor of the inverter system reach which is 98% of the power extracted. The ripple voltage at MPP should not exceed 6.5% compared to nominal output voltage. The FLC and ANFIS simulated output are shown in Fig. 15. ISSBC inverter exhibits higher efficiency of 2-5% over the conventional boost inverter.

7.5. Effect of Partially Shaded Solar Irradiation

Finally, in order to verify the performances of the FLC and ANFIS algorithm, the CHBMLI is connected to an RL load (R=100 ohm and L=20mH) using switching frequency of 30 kHz in the ISSBC. Under balanced condition both PV arrays receives constant solar irradiation of 1000W/m^2. The DC voltage input of four H-bridge inverter are V_{dc1}=V_{dc2}=52 V and under unbalanced condition the two PV array irradiation of 1000W/m^2 and 800 W/m^2 respectively. The DC voltage input of four H-bridge inverter, for example, may become V_{dc1}=52V and V_{dc2}=46V respectively. The output of the step modulated inverter, both voltage and current, along with their harmonic spectrum up to 7.5 kHz under balanced condition for the FLC and ANFIS algorithms are shown in Fig.16 (a-d) and Fig.17 (a-d), respectively. The total harmonic distortion (THD) of the output voltage and current with the FLC model of control are 29.54% and 8.39% and with the ANFIS model they are 25.62% and 7.39% respectively. Similarly, under the unbalanced operating conditions of the PV panels both algorithms exhibit THD values for voltage and current as shown in Fig.18 (a-d) and Fig 19 (a-d) respectively. The total harmonic distortion (THD) of the output voltage and current in the case of FLC is 28.69% and 7.64%respectively.

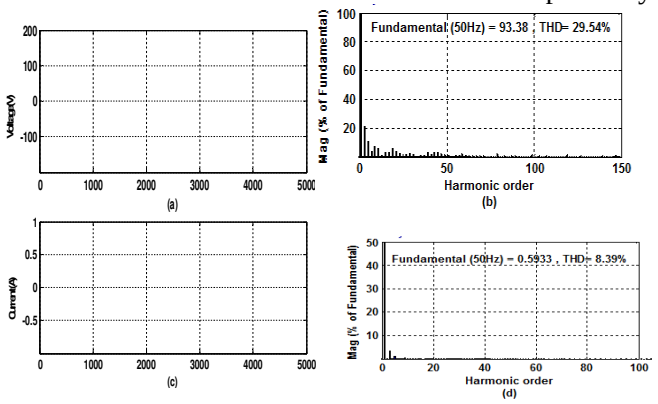

Fig.16.Simulation results for FLC MPPT under balanced condition (a) output voltage (b) voltage harmonic spectrum (c) out current (d) current harmonic spectrum

With the ANFIS model the THD values for voltage and current are 27.22% and 6.45% respectively. It can be observed from the simulation results that for both

balanced and unbalanced conditions, the percentage THD is less in ANFIS algorithm as compared to the FLC algorithm.

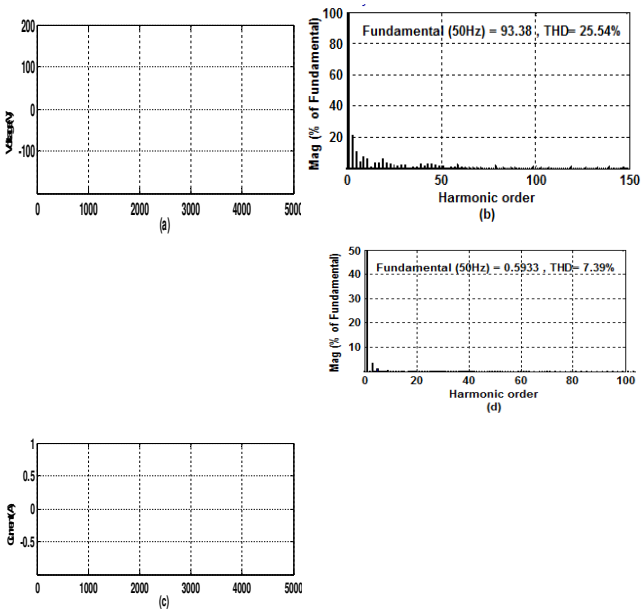

Fig.17 Simulation results for ANFIS MPPT under balanced condition (a) output voltage (b) voltage harmonic spectrum (c) out current (d) current harmonic spectrum

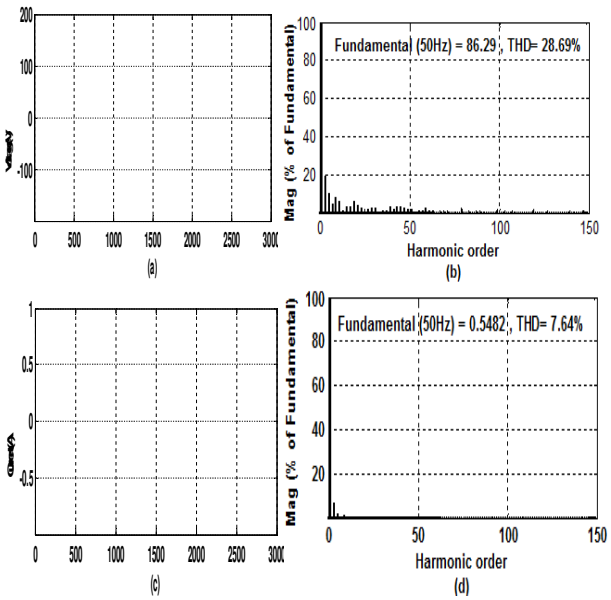

Fig.18.Simulation results for FLC MPPT under unbalanced condition (a) output voltage (b) voltage harmonic spectrum (c) out current (d) current harmonic spectrum

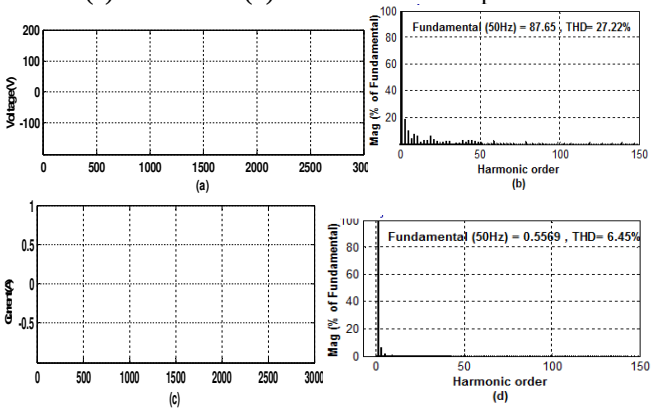

Fig.19.Simulation results for ANFIS MPPT under unbalanced condition (a) output voltage (b) voltage harmonic spectrum (c) out current (d) current harmonic spectrum

8. Experimental validation

The simulation results were verified experimentally in the using the appropriate hardware built around the PIC 16F877A microcontroller. The proposed system was tested in the laboratory and the photograph of the experimental setup that includes the 16F877A microcontroller is shown in Fig. 20 (a-b). The solar panels are not shown in photograph. The controller program is downloaded into 16F877A microcontroller and generates gating signals to the ISSBC and CHBLI. The MPPTs extracted power can be observed as an exposition of approximately 04:00 hrs range from 09:00 hrs to 14:00 hrs with different PV insulation and cell temperature under partially shading condition. To investigate the performance of the proposed single phase CHBMLI based standalone PV system a prototype model is developed as explained in section-6. For the experimental validation, at different time, intervals the output voltage and current of the PV module under different load and atmospheric conditions are noted down and for the corresponding values of the PV current and voltage characteristic curves are plotted and this is shown in Fig.21 and Fig.22 respectively. The Fig.21 and Fig.22 shows the Voltage vs. Current characteristics and voltage vs. Power characteristics of the PV module. From these

characteristic curves, the maximum power point at different atmospheric condition can be estimated. For the validation of maximum power point tracking control, the developed DC-DC inverter is tested on at 1:15 PM**.** The irradiation and temperature were measured as 1050 Watt/m^2 and 35°C respectively. During experimentation, both the PV modules in balanced condition with FLC and ANFIS algorithm generates Vdc1=Vdc2= 48.71V and Vdc1=Vdc2=52.31V respectively. The UNI –T four channels DSO was used to take the voltage waveform with their harmonic spectrum. Similarly, under balanced operation the rms value of output voltage is found as 70.76 and 72.14 Volts respectively.

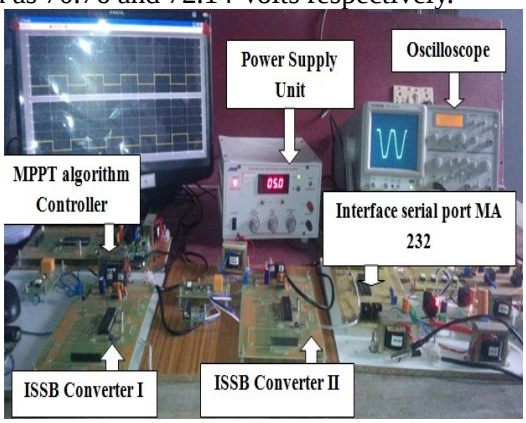

Fig.20. Experimental arrangement (a) ISSBC

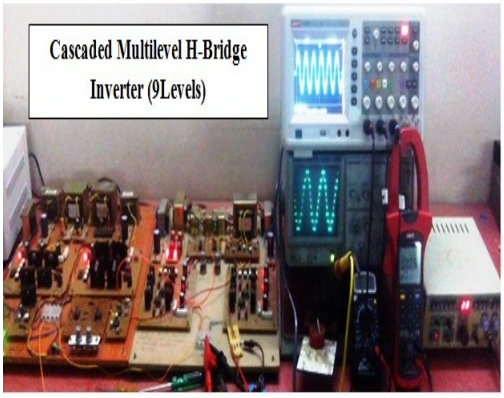

Fig.20. Experimental arrangement (b) CHBMLI (nine levels)

Fig 23 (a) and (b) shows the voltage and harmonic spectrum and the corresponding THDs which are found to be 12.3 % and 10.3 % respectively. In order to test the algorithm for unbalanced condition, intentionally one of the PV modules was shaded by 20 %. Under this condition, the partially shaded module with FLC and ANFIS algorithms are generating Vdc2=37.55 V and Vdc2=43.8 V respectively.

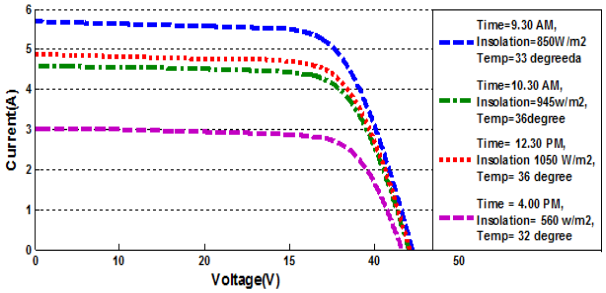

Fig.21. V and I characteristics of PV module based on experimental data

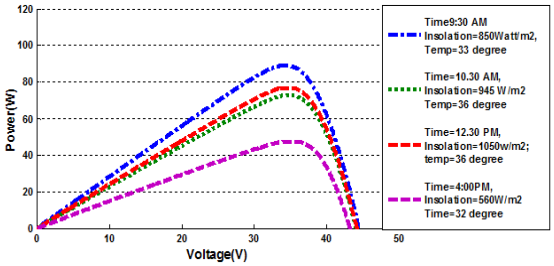

Fig.22. P and V characteristics of PV module based on experimental data

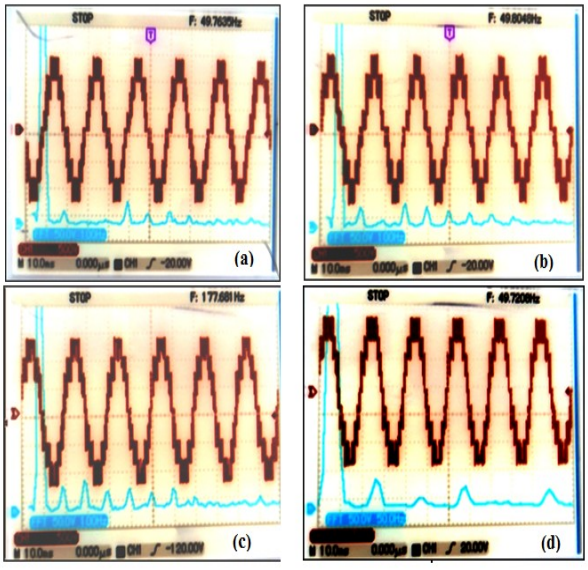

Fig.23. Experimental result for (a) balanced ANFIS output voltage and harmonic spectrum (b) balanced FLC voltage

harmonic spectrum (c) unbalanced ANFIS out voltage and harmonic spectrum (d) unbalanced FLC out voltage and harmonic spectrum

Under unbalanced conditions prevailing over the PV panels in terms of insulation because of partial shadows the output voltage with their corresponding harmonic spectrums is shown in Fig.23 (c) and (d). The rms value of output voltage 69.41V and 71.32V and the corresponding THDs are found to be at 16.4 % and 12.7 %. As the number of levels is increased even under the unbalanced condition the output voltage quality gets improved significantly. Hence, in both balanced and partially shaded operation modes, ANFIS algorithm improves the voltage quality, power extraction, harmonics elimination as compared to the FLC algorithm.

9. Conclusion

This paper analyzes the performance of FLC and ANFIS MPPT algorithms by stand-alone PV system. The configuration for the proposed system is designed and simulated using MATLAB/Simulink and implemented in 16F877A microcontroller. The acceptable results are summarized as follows. The proposed system shows a good dynamic performance algorithm to track the MPP of the PV units even under the rapid change of the irradiation and cell temperature. It has been observed that the ISSBC can be more efficient than the conventional controllers due to fast prototyping, software design and simple hardware design giving maximum efficiency at all load conditions. In this study non isolated interleaved boost inverter is selected to achieve low cost, simple control structure and high efficiency. The ISSBC with ANFIS can provide the overall efficiency higher than FLC algorithms. The CHBMLI integrate with SHE FLC modulation technique improved output voltage quality and reduction in THD percentage even in unbalanced insulation of PV modules with the ANFIS based MPPT algorithm. The results obtained show the ANFIS model of controller can gain importance in high performance applications such as PV generation system.

References

[1] Xianwen Gao., Shaowu Li., Rongfen Gong., Maximum power point tracking control strategies with variable weather parameters for photovoltaic generation systems, Solar Energy, 93 (5), 357-367, 2013

[2] Kashif Ishaque., Zainal Salam., A Deterministic particle swarm optimization maximum power point tracker for photovoltaic system under partial shading condition IEEE Transactions on Industrial Electronics, 60 (8), 3195-3206, 2013

[3] Valan Rajkumar.M., Manoharan.P.S., FPGA based multilevel cascaded inverters with SVPWM algorithm for photovoltaic system, Solar Energy, 87 (1), 229-245, 2013

[4] Yi-Hua Liu., Chun-Liang Liu., Jia-Wei Huang., Jing-Hsiau Chen., Neural-network-based maximum power point tracking methods for photovoltaic systems operating under fast changing environments, Solar Energy, 89 (5), 42-53, 2013

[5] Tsang.K.M., Chan.W.L., Three-level grid-connected photovoltaic inverter with maximum power point tracking, Energy Conversion and Management, 65 221-227, 2013

[6] Ratna Ika Putri., Rifa.M., Maximum power point tracking control for photovoltaic system using neural fuzzy, International Journal of Computer and Electrical Engineering, 4 (1), 75-81, 2012

[7] Azadeh Safari., Saad Michele., Simulation and hardware implementation of incremental conductance MPPT with direct control method using cuk inverter, IEEE Transactions on Industrial Electronics, 58 (4), 1154-1161, 2011

[8] Chokri Ben Salah., Mohamed Ouali., Comparison of fuzzy logic and neural network in maximum power point tracker for PV systems, Electric Power Systems Research, 81, 43-50, 2011

[9] Mellit.A, Kalogeria SA., ANFIS-based modeling for photovoltaic power supply system. Renewable Energy 36 (1) 250–258, 2011

[10] Ravi.A., Manoharan.P.S., Vijay Anand.J., Modeling and simulation of three phase multilevel inverter for grid connected photovoltaic systems, Solar Energy, 85(11), 2811-2819, 2011

[11] Doo-Yong Jung., Young-Hyok Ji., Sang-Hoon Park., Yong Chae Jung., Chung-Yuen Won., Interleaved Soft-Switching boost inverter for photovoltaic power-generation system, IEEE Transactions on Power Electronics, 26 (4), 1137-1145, 2011

[12] Malla.S.G., Bhende.C.N., Mishra.S, Photovoltaic based water pumping system, the school of electrical sciences, Indian Institute of Technology Bhubaneswar, IEEE Conference, 978-1-4673-0136-7/11., 2011

[13] Faete Filho., Leon.M., Tolbert., Yue Cao., Real-time selective harmonic minimization for multilevel inverters connected to solar panels using artificial neural network

angle generation, IEEE Transactions on Industry Applications, 47 (5), 2117-2124, 2011
[14] Whei-Min Lin., Chih-Ming Hong., Chiung Hsing Chen., Neural network based MPPT control of a stand-alone hybrid power generation system, IEEE Transactions on Power Electronics, 26 (12), 3571-3581, 2011
[15] Beser.E., Arifoglu.B., Camur.S., Beser.E.K.,A grid-connected photovoltaic power conversion system with single-phase multilevel inverter, Solar Energy, 84 2056-2067, 2010
[16] Taufik., Akihiro oi., Makbul Anwari Mohammad Taufik., Modeling and simulation of photovoltaic water pumping system, Third Asia International Conference on Modeling & Simulation, 2009
[17] Leon.J.I, Vazquez.S, Watson A.J, Franquelo L.G, Wheeler.P.W, J.M. Carrasco.J.M. Feed forward space vector modulation for single-phase multilevel cascaded inverters with any DC voltage ratio, IEEE Transactions on Industrial Electronics, 56 315-325, 2009
[18] Patel.H V., Agarwal.V., MATLAB based modeling to study the effects of partial shading on PV array characteristics, IEEE Transaction on. Energy Conversion, 23, 302, 2008
[19] Jun-Ho Kim., Doo-Yong Jung., Jae-Hyung Kim., Su-Won Lee., Yong-Chae Jung., Chung-Yuen Won., Soft switching interleaved boost inverter for photovoltaic, power generation system, ICSET, 257-262, 2008
[20] Esram.T., Chapman.P.L., Comparison of Photovoltaic array maximum power point tracking techniques, IEEE Trans. Energy Conversion, 22 (2), 439-449, 2007
[21] Hohm.D.P., Ropp.M.E, Comparative study of maximum power point tracking algorithms using an experimental, programmable, maximum power point tracking test bed, Proc. Photovoltaic Specialist Conference, 1699-1702, 2000